JOURNAL OF COMPUTATIONAL PHYSICS **135,** 189–197 (1997)
ARTICLE NO. CP975701

Numerical Simulation of Hydrodynamics by the Method of Point Vortices

J. P. Christiansen

UKAEA Research Group, Culham Laboratory, Abingdon, Berkshire, England

Received October 14, 1971

The motion of a two-dimensional incompressible inviscid and homogeneous fluid can be thought of in terms of the gradual evolution of a continuous vorticity distribution, each scalar vortex element interacting with every other by an instantaneous action at a distance law. It is of particular interest that this model can be expressed in Hamiltonian form and that it shows many analogies with similar systems in plasma physics. In addition to the standard mesh techniques, a computational description can be obtained if the continuous vorticity distribution is replaced by a finite set of point vortices interacting through a stream function which satisfies Poisson's equation. The point vortices move in a velocity field given on a Cartesian mesh such that there is a close resemblance to particle models used in plasma simulations. The point vortex model is presented with a calculation on a test model and the sources of numerical errors are explained. Graphical results from several calculations are shown and it is concluded that the point vortex model is useful and versatile for a variety of problems in hydrodynamics as well as in plasma physics.

1. INTRODUCTION

Incompressible fluid flows have been the subject of many investigations. Although the nonlinearity of the partial differential equations renders them insolvable except for special cases, many of the most interesting flow properties can only be explained through the nonlinearity. The advent of computers has over the last two decades made it a challenging problem to study fluid flows in the nonlinear regime by applying suitable numerical techniques. So far efforts have mainly been concentrated on systems of one or two dimensions because of computer storage requirements. A very useful annotated bibliography of numerical methods used in fluid dynamics has recently been compiled by Harlow [1].

This paper is concerned with incompressible, inviscid flows in two dimensions satisfying the Euler equations for an ideal fluid of uniform density

$$\nabla \cdot \mathbf{u} = 0, \tag{1}$$

Reprinted from Volume 13, Number 3, November 1973, pages 363–379.

$$\partial \mathbf{u}/\partial t + \mathbf{u} \cdot \nabla \mathbf{u} = -1/\rho \nabla P, \tag{2}$$

where $\mathbf{u}$, ρ, and P denote fluid velocity, density, and pressure, respectively. Provided that no free surfaces are present it is convenient to eliminate these primitive variables, introducing the vorticity $\boldsymbol{\zeta}$ and stream function $\boldsymbol{\psi}$ according to

$$\boldsymbol{\zeta} = \nabla \times \mathbf{u}, \quad \mathbf{u} = \nabla \times \boldsymbol{\psi}. \tag{3}$$

For a two-dimensional flow field we can consider $\boldsymbol{\zeta} = (0, 0, \zeta)$ and $\boldsymbol{\psi} = (0, 0, \psi)$ as scalars and Eqs. (1) and (2) then become

$$\partial \zeta/\partial t + [\zeta, \psi] = 0, \tag{4}$$

$$\nabla^2 \psi = -\zeta, \tag{5}$$

where for any two scalars A and B

$$[A, B] \equiv \frac{\partial A}{\partial x}\frac{\partial B}{\partial y} - \frac{\partial B}{\partial x}\frac{\partial A}{\partial y}. \tag{6}$$

Equations (4) and (5) can, of course, be solved by Eulerian mesh techniques and many such calculations have been carried out, notably by Fromm. Section IIIA of Ref. [1] gives a list of references to this and other work. For sufficiently simple geometry, a considerable improvement in speed can be obtained by using a fast Fourier transform [2, 3] or similar technique to solve Poisson's equation (5).

The method of solution used by Christiansen and Roberts [4] and described in this paper differs from those commonly adopted in numerical hydrodynamics, and more closely resembles the particle simulation techniques employed in plasma physics [5]. It starts from a physical model in which the continuous vorticity distribution $\zeta(x, y)$ is approximated by a large number of point vortices

$$\zeta = \sum_{n=1}^{N} \zeta_n \delta(x - x_n)\, \delta(y - y_n), \tag{7}$$

0021-9991/97 $25.00

where $\zeta_n = +1$ or -1. Each pair of coordinates (x_n, y_n) is called a point vortex and satisfies the equations of motion

$$\dot{x}_n = \frac{\partial \psi}{\partial y_n}, \quad \dot{y}_n = -\frac{\partial \psi}{\partial x_n}, \tag{8}$$

where ψ is a solution of Poisson's equation (5)

$$\psi = \frac{1}{2\pi} \sum_{\substack{n=1 \\ (n \neq m)}}^{\infty} \sum_{m=1}^{\infty} \zeta_n \zeta_m \log r_{nm} \tag{9}$$

with

$$r_{nm}^2 = |\mathbf{r}_n - \mathbf{r}_m|^2, \tag{10}$$

the infinite self energy of each point vortex being excluded.

Groups at Livermore, Los Alamos, Stanford, Princeton, and elsewhere have developed a variety of numerical techniques for particle simulation in plasma physics, and calculations have been reported by Birdsall, Fuss, Byers, Morse, Hockney, Dawson, and others. Reference [5] provides a recent account of this work. There are interesting analogies [6] between the incompressible flow of a real hydrodynamic fluid in two-dimensional (x, y)-space, and the incompressible flow of a "phase fluid" in the two-dimensional (q, p)-space which is used to describe a collisionless plasma satisfying the Valasov equation.

The hydrodynamic program VORTEX which is discussed in this paper has in fact been used by Taylor and McNamara [7] to study two-dimensional guiding center problems in a magnetized plasma which are formally identical to those of an ideal fluid, whilst the hydrodynamic flows depicted in Fig. 5 (rows 1 and 3) were previously studied in the plasma case by Byers [8] and Hockney [9], and by Birdsall and Fuss [10], respectively. These authors included a finite Larmor radius, but despite these and other differences our results agree qualitatively with theirs.

One reason why vortices are important in hydrodynamics is that they are the *sources* for the incompressible flow field; if we are given the vorticity distribution at any instant of time then both the current state of the system and its future evolution are in principle determined subject to appropriate boundary conditions. This property is reminiscent of any Hamiltonian system, and it can indeed be shown that Eqs. (4) and (5) can usefully be expressed in Hamiltonian form. Another obvious analogy is with interacting electrical point charges or gravitating masses by virtue of Poisson's equation. This suggests that an incompressible flow field should be thought of in terms of the mutual interaction of a set of vortex elements (action-at-a-distance model), rather than in terms of the velocity field itself (field model), and a much clearer picture of the flow is often obtained in this way. Point vortex models have been used in numerical calculations by several authors, as for example by Abernathy and Kronauer [11], who studied the formation of the von Kármán vortex street, and Chorin [12], who used point vortices for studies of slightly viscous flows.

It is of great interest to study quite simple flow configurations in two dimensions in order to acquire a fundamental understanding of the dynamics of nonlinear flows. In Figs. 5 and 6 we show seven examples of hydrodynamic systems to emphasize the complexity of nonlinear processes. These seven systems have been simulated using the numerical techniques discussed in this paper. The state of the system at time t may be represented by a set of contours $\zeta(x, y, t) =$ constant, and according to Eq. (4) these move with the fluid, the area between any pair of contours remaining constant with time. Step-function or "waterbag" distributions in which the contours enclose regions of uniform vorticity $\zeta = \pm\zeta_0$ are of particular interest.

To interpret the phenomena that we discover from any type of numerical simulation it is necessary to understand in detail the errors which are introduced by replacing the partial differential equations by their finite difference equivalents. These errors can most easily be determined by comparing the numerical solutions of simple well-known problems with their analytic counterparts. Any anomalies such as numerical viscosity which are contained within the difference scheme will then appear in an obvious way. In this paper we describe the numerical scheme which is used to follow the motion of an assembly of point vortices. This numerical scheme is applied to a simple test problem described in Sections 4 and 5. The results from calculations on the test problem are presented and analyzed. In the last section we outline the deficiencies of the numerical scheme as well as the motivations for using it.

2. A NUMERICAL SCHEME FOR THE MOTION OF POINT VORTICES

Suppose we are given an ensemble of N point vortices with coordinates (x_n, y_n) lying inside a rectangular region covered by a Cartesian mesh of size N_x by N_y. To evaluate the vorticity $\zeta(i, j)$ at the mesh point (i, j) we use the cloud-in-cell (CIC) method [13]. This method assumes each "point" vortex to possess uniform vorticity within a unit square such that the corresponding unit amount of vorticity can be credited to surrounding mesh points through a bilinear interpolation. A smoothing of the vorticity distribution will result from the bilinear interpolation, and Section 6 describes the numerical effect of this.

Let us assume that the coordinates of a point vortex are written as $x_n = i + dx$ and $y_n = j + dy$. The CIC method credits vorticity to the four surrounding mesh-points by

$$\begin{aligned}\zeta(i,j) &= (1-dx)(1-dy) = A_1,\\ \zeta(i+1,j) &= dx(1-dy) = A_2,\\ \zeta(i,j+1) &= (1-dx)\,dy = A_3,\\ \zeta(i+1,j+1) &= dx\,dy = A_4.\end{aligned} \tag{11}$$

The quantities A_1–A_4 represent four areas of intersection between the mesh and the square-shaped vortex, and the CIC method is often referred to as the area-weighting technique. When the vorticity from all N point vortices has been credited to the mesh points using (11), Poisson's equation (5) can be solved by the usual five-point approximation

$$\frac{\psi(i,j+1)+\psi(i,j-1)-2\psi(i,j)}{(\Delta y)^2} + \frac{\psi(i+1,j)+\psi(i-1,j)-2\psi(i,j)}{(\Delta x)^2} = -\zeta(i,j), \tag{12}$$

where $\Delta x, \Delta y$ are the mesh spacings. Equation (12) is solved by the Hockney method [14] allowing for a variety of boundary conditions. The velocity field is evaluated by centered differences

$$\begin{aligned}u_x(i,j) &= \frac{\psi(i,j+1)-\psi(i,j-1)}{2\,\Delta y};\\ u_y(i,j) &= -\frac{\psi(i+1,j)-\psi(i-1,j)}{2\,\Delta x}.\end{aligned} \tag{13}$$

To advance the set of positions (x_n, y_n) one timestep, a leapfrog scheme is used. Two sets of coordinates $(x_n, y_n)_{\text{even}}$ and $(x_n, y_n)_{\text{odd}}$ are introduced in order to express the coordinates at alternate times $2s\ \Delta t$ and $(2s+1)\ \Delta t$. The equations

$$\dot{x}_n = u_x, \quad \dot{y}_n = u_y$$

then become, letting superscript s denote the time $s\ \Delta t$,

$$\begin{aligned}x_n^{s+1} &= x_n^{s-1} + u_x^s(x_n^s, y_n^s)\,2\,\Delta t,\\ y_n^{s+1} &= y_n^{s-1} + u_y^s(x_n^s, y_n^s)\,2\,\Delta t.\end{aligned} \tag{14}$$

The set of coordinates (x_n^s, y_n^s) determines the velocity field (also ζ^s, ψ^s) which is used to move the other set. The velocity $\mathbf{u} = (u_x, u_y)$ used in (14) is evaluated by the CIC method according to

$$\begin{aligned}\mathbf{u}(x_n^s, y_n^s) = {} & A_1^s\mathbf{u}(i,j) + A_2^s\mathbf{u}(i+1,j)\\ & + A_3^s\mathbf{u}(i,j+1) + A_4^s(\mathbf{u}(i+1,j+1)),\end{aligned} \tag{15}$$

where the four areas A_1^s–A_4^s at time $s\ \Delta t$ are given by (11). Equations (11) and (15) form a consistent set of interpolations in the sense that a single point vortex will not move in its own velocity field.

3. THE VORTEX COMPUTER CODE

The computer code VORTEX [15] solves Eqs. (11)–(14) on a square mesh with $N_x = N_y = 64$ and $\Delta x = \Delta y = 1$. Part of the code is the Hockney–Poisson solver POT1 [14] which allows nine different sets of boundary conditions in x and y. Only two of these nine sets have been used for the flows of Figs. 5 and 6. The stream function is in the first case assumed constant along the square boundary. In the second case ψ is periodic in x and constant along the y-boundaries. The computing time used to implement the sequence (11)–(14) depends on the boundary conditions. On an ICL KDF9 computer (equivalent to an IBM 7090) it took 2.5 sec to advance the positions of 3200 point vortices (negative or positive) when ψ is constant along the boundary. Most of this time (approx. 10 sec) was taken up by solving Poisson's equation while Eq. (14) was solved by a fast vector integration technique described by Roberts and Boris in an earlier paper [16].

The dynamics of the flows shown in Figs. 5 and 6 have been analyzed by the author [17]. This reference also describes the effects caused by the finite difference formulation, i.e., the use of finite values of N, Δx, Δy, and Δt. The VORTEX code has in addition been used extensively to study two-dimensional guiding center plasmas by Taylor and McNamara [7] and by Christiansen and Taylor [18]. The motion of guiding centers for ions and electrons is identical to that of positive and negative point vortices, respectively, and in these calculations the electrostatic potential φ which is identical to the stream function ψ is assumed periodic in both x and y.

4. PROPERTIES OF THE TEST SYSTEM

To obtain a quantitative measure of the effects of the approximations made in Eqs. (11)–(15) we apply the numerical scheme described in Section 2 to a simple and fully understood flow problem. By choosing a time-independent flow as a test problem for the scheme we can be sure that any time variation occurring in the numerical results must be ascribed to the approximations made.

A circular region of radius R_0 and $\zeta = \zeta_0$ with $\zeta = 0$ elsewhere is called Rankine's combined vortex [19, 20], when the solutions to Poisson's and Laplace's equations inside and outside the circle, respectively, are fitted properly at $r = R_0$

$$\begin{aligned}\psi &= \psi_0 - \tfrac{1}{4}\zeta_0(r^2 - R_0^2) \qquad r \le R_0,\\ \psi &= \psi_0 - \tfrac{1}{4}\zeta_0 R_0^2 \log r/R_0 \quad r \ge R_0.\end{aligned} \tag{16}$$

The fluid velocity is everywhere azimuthal

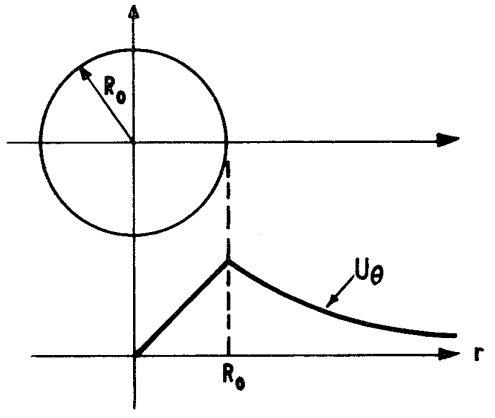

FIG. 1. Rankine's combined vortex as test model.

$$\begin{aligned} u_r &= 0, \\ u_\theta &= \tfrac{1}{2}\zeta_0 r \qquad r \le R_0, \\ u_\theta &= \tfrac{1}{2}\zeta_0 (R_0^2/r) \quad r \ge R_0, \end{aligned} \tag{17}$$

which is indicated in Fig. 1. Since the vorticity ζ is a function of the stream function ψ only, i.e., $\zeta = \zeta(\psi)$, we have a steady-state flow as the Poisson bracket $[\zeta, \psi]$ of Eq. (4) is zero. Rankine's combined vortex is an analytic approximation to a motion often encountered in real fluids, although the viscous effects present in real fluids will eventually smooth out the discontinuous ζ distribution, vorticity diffusing through the surrounding irrotationally moving fluid according to $d\zeta/dt = \nu\nabla^2\zeta$ so that the vortex decays exponentially and in the limit $t \to \infty$ the flow is fully irrotational [21].

If a small-amplitude irrotational disturbance

$$\Delta\psi = A_m e^{i(m\theta - \omega_m t)} \begin{Bmatrix} r^m & r \le R_0 \\ r^{-m} & r \ge R_0 \end{Bmatrix} \tag{18}$$

is imposed it will cause a stable azimuthal corrugation to travel around the interface $r = R_0$ with an angular velocity [19]

$$\omega_m/m = \tfrac{1}{2}\zeta_0((m-1)/m). \tag{19}$$

The steady-state flow is, thus, linearly stable, an important feature in view of the results presented in Section 6.

5. THE SET-UP FOR NUMERICAL SIMULATION

To obtain a circular region of constant $\zeta = \zeta_0$ we distribute point vortices as shown in Fig. 2. On J rings of radii $r_j = jd$, $j = 1, J$ we place point vortices at angles $\theta_{ij} = i(2\pi/jM)$, $i = 1, jM$. This distribution credits a constant area $\pi d^2(2J/(J+1)M)$ to each point vortex.

In the experiments we set $d = 0.3$, $J = 24$, $M = 10$. The total number of particles is 3,000 plus two particles in the center. The area is 163 and the period of rotation is $T_0 = 4\pi/\zeta_0 = 0.682$. We have chosen $\Delta t = 16/3002$, such that the approximate number of timesteps for one rotation is 128. The maximum velocity occurring at $r = R_0$ is $V_{\max} = \frac{1}{2}\zeta_0 R_0 = 66.4$ so that the Courant–Friedrichs–Lewy condition is satisfied ($V_{\max}\,\Delta t = 0.35$).

A system of point vortices resembling the arrangement in Fig. 2 has been examined by Morikawa and Swenson [22]. They study N point vortices, geostrophic or logarithmic, distributed on a circle. Their stability analysis of this system is already quite complex as N varies from 2 to 10, and with 24 rings present in our experiment we shall make no attempt to analyze the stability.

In the first series of experiments we place the vortex made up of particles in the center of a square mesh and normally restrict ψ to be a constant (0) along the perimeter of the square. The simulation is run for about 1,000 timesteps. Ideally all jM point vortices on ring j should remain on this ring. To see whether this is the case we define the radius function for ring j as

$$r_j(\theta) = |\mathbf{r}_n - \mathbf{r}_g|,$$

where $\mathbf{r}_g$ is the fixed center of gravity of the jM points on ring j

$$\mathbf{r}_g = 1/jM \sum_{n=1}^{jM} \mathbf{r}_n.$$

The radius function can be represented by a finite Fourier series

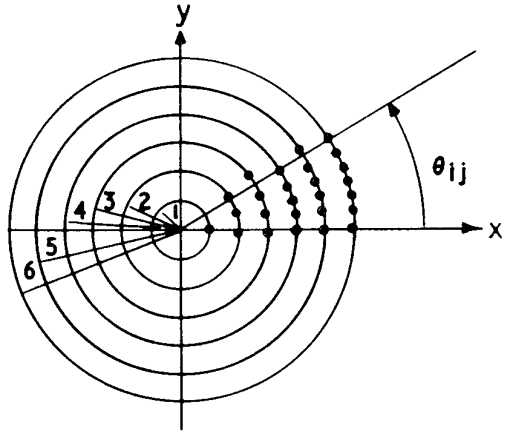

FIG. 2. Point vortices arranged to simulate Rankine's combined vortex.

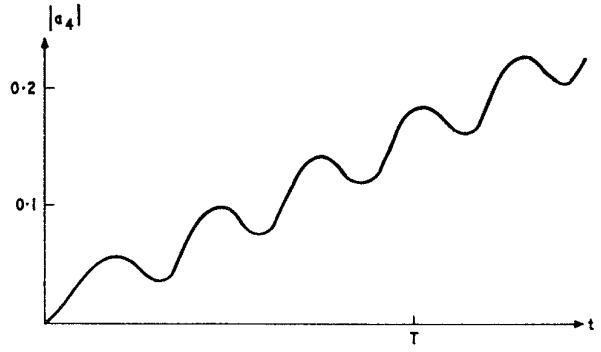

FIG. 3. Amplitude of the $m = 4$ azimuthal mode versus time, measured at $r = 7.2$.

$$r_j(\theta) = \sum_{m=2}^{L} a_m e^{im\theta}, \tag{20}$$

where a_m is complex. Evidently $a_0 = a_1 = 0$. Since at $t = 0$, $a_m = 0$ for all m any development of an azimuthal mode will represent effects that are due to the finite difference formulation or the arrangement of points as explained above.

Analysis of the positions $\mathbf{r}_i$, $i = 1, jM$ provides us with a_m $(m = 1, 16)$ as well as the perimeter and area enclosed by the curve they define. We have carried out seven numerical experiments as outlined below. In these experiments we try to eliminate the effects from each of the approximations (12)–(15).

Experiment 1: Standard experiment on the vortex as described above.

Experiment 2: Along the square boundary ψ becomes a function of the distance from the center of the vortex.

Experiment 3: Δt is varied.

Experiment 4: A single ring of radius $R_d = 6.0$ is moved in a time independent velocity field inherited from Experiment 1.

Experiment 5: As Experiment 4 but with $R_d = 7.2^2/6.0$.

Experiment 6: As Experiment 4 but with $R_d = R_0 = 7.2$.

Experiment 7: Repeats of Experiments 4–6 but with an analytic velocity field.

6. RESULTS FROM THE CALCULATIONS

The results from Experiment 1 reveal an anomalous instability: The azimuthal modes a_4, a_8, a_{12}, ... (Eq. (20)) grow with time as shown in Fig. 3 for a_4. All other modes remain at the level of rounding off errors. The area of the vortex, the total kinetic energy, and the angular momentum which are invariants of motion [17] are conserved to within rounding off errors. In [17] it is shown that the presence of a square and fixed boundary changes the stream function (Eq. (16)) by $\delta\psi$ where

$$\delta\psi = \sum_{-\infty}^{\infty} b_m e^{im\theta} = \sum_{\substack{-\infty \\ m\neq 0}}^{\infty} \zeta_0 R_0^2 \frac{1}{8m}\left(\frac{r}{2L}\right)^{4m} e^{i4m\theta}. \tag{21}$$

L is the dimension of the square. $\delta\psi$ is a disturbance of the type given by Eq. (18) and it causes *stable* modes a_{4m} to oscillate with an ω_m given by Eq. (19). The amplitudes a_m are related to the coefficients b_m of Eq. (21) by [19]

$$a_m = (2m/\zeta_0)b_m.$$

With our data $a_4 \simeq 10^{-5}$. The rounding off errors are of the order 10^{-5} (in cell length units) corresponding to 18 bits [16]. Thus, the square fixed boundary cannot cause the amplitudes a_{4m} to grow and Experiment 2 verifies this.

The leapfrog time integration method (Eq. (14)) can cause numerical instabilities when the two time levels get out of step. We have, however, devised a method [15] of suppressing such a tendency. In Experiment 3 this method is applied at a variable frequency for several calculations and different values of Δt are also used. However, the azimuthal modes develop as they did in Experiment 1.

In Experiments 4–6 we eliminate the solution of Poisson's equation (Eq. (12)) and the difference form (Eq. (13)) by moving a ring of particles in the $t = 0$ velocity field of Experiment 1. The motion follows Eqs. (14) and (15). It is found in Experiment 4 that a_{4m} oscillate with the frequencies given by Eq. (19) as shown in Fig. 4 for a_4. Experiments 5 and 6 produce the growth of Experiment 1.

Finally, to eliminate possible errors in the $t = 0$ velocity field calculated in Experiment 1, we repeat Experiments 4–6, this time (Experiment 7) with the analytic velocity field of Eq. (17). Experiment 7 demonstrates that the area weighting method is exact when $r > R_0$ since then the velocity varies linearly with r. For $r > R_0$ the interpolation

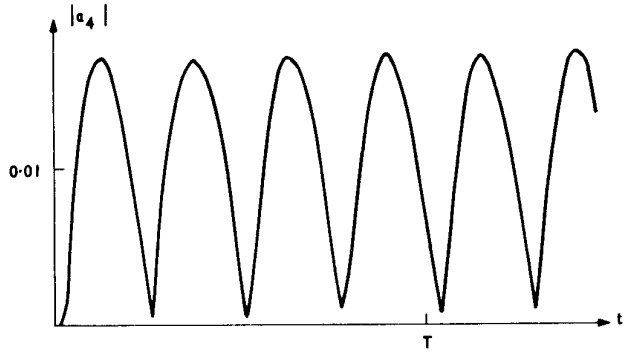

FIG. 4. Amplitude of the $m = 4$ azimuthal mode versus time, measured at $r = 6.0$.

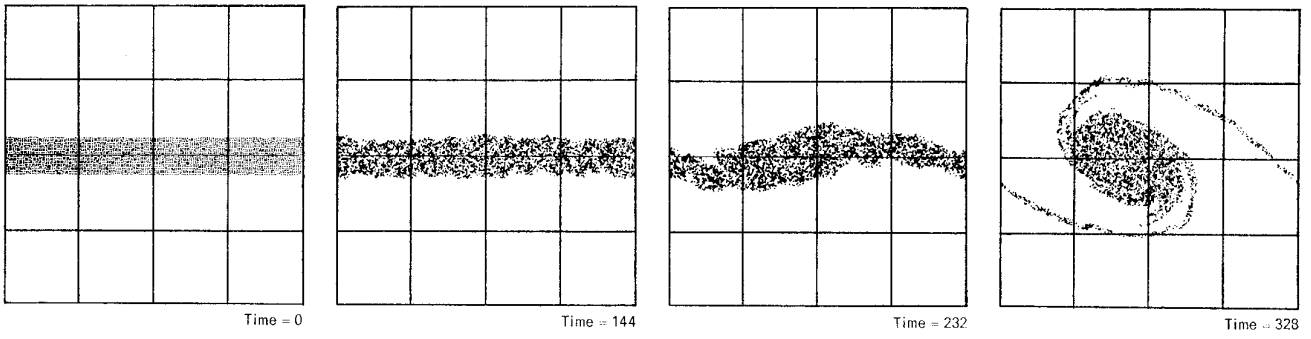

The onset of the Kelvin-Helmholtz instability.

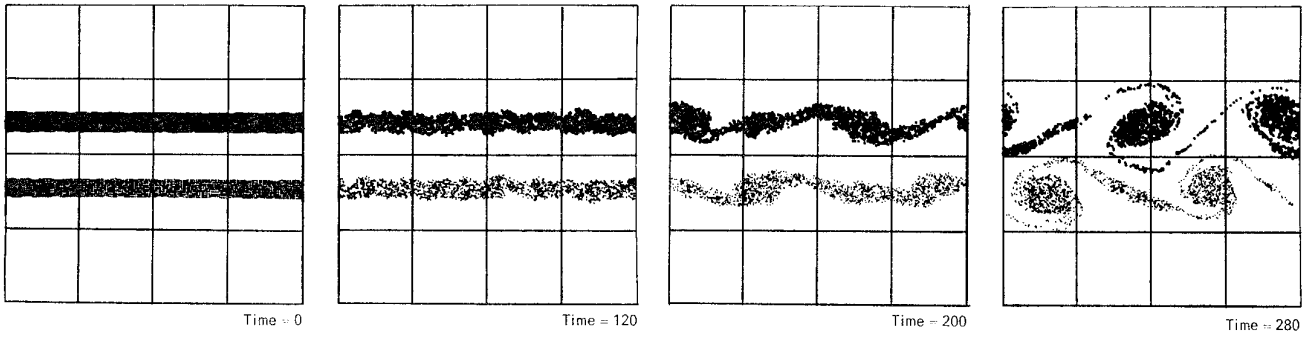

The formation of the von Karman vortex street.

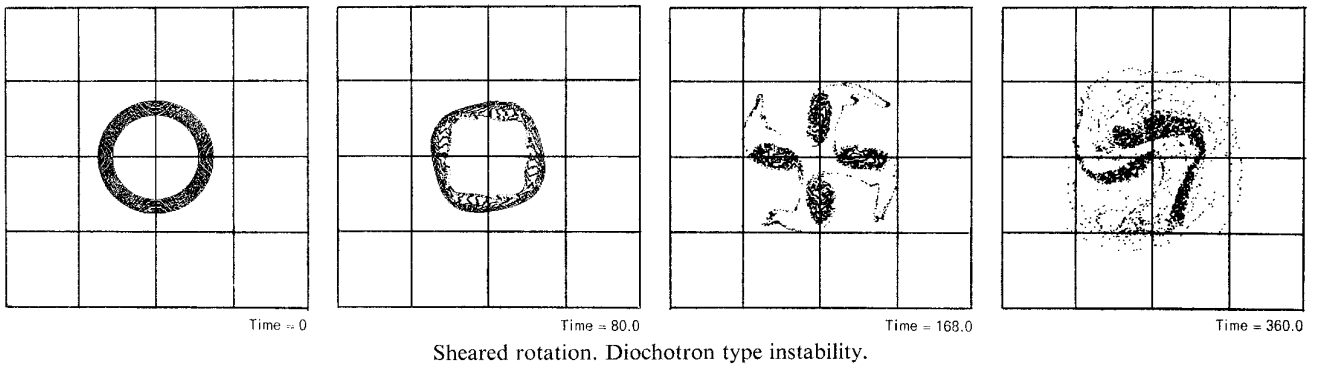

Sheared rotation. Diochotron type instability.

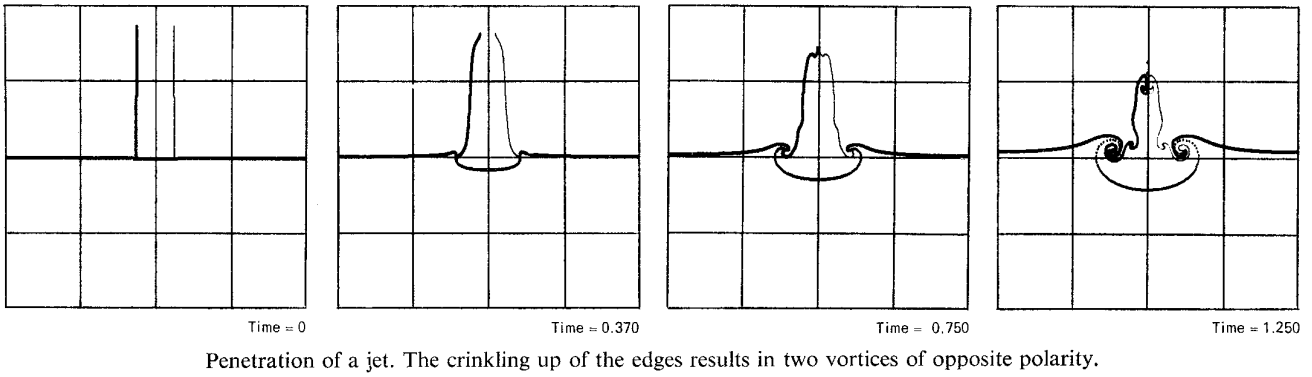

Penetration of a jet. The crinkling up of the edges results in two vortices of opposite polarity.

FIG. 5. Flow problems simulated by program VORTEX.

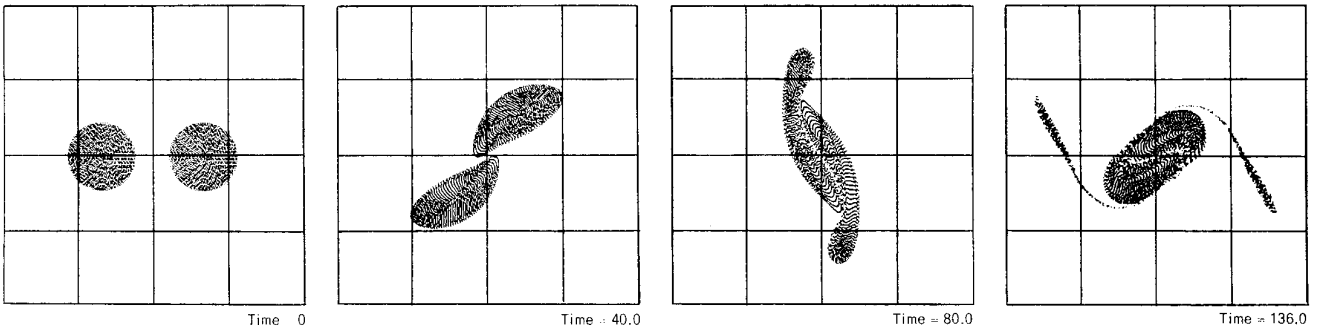

Two vortices coalescing because of sufficient initial proximity.

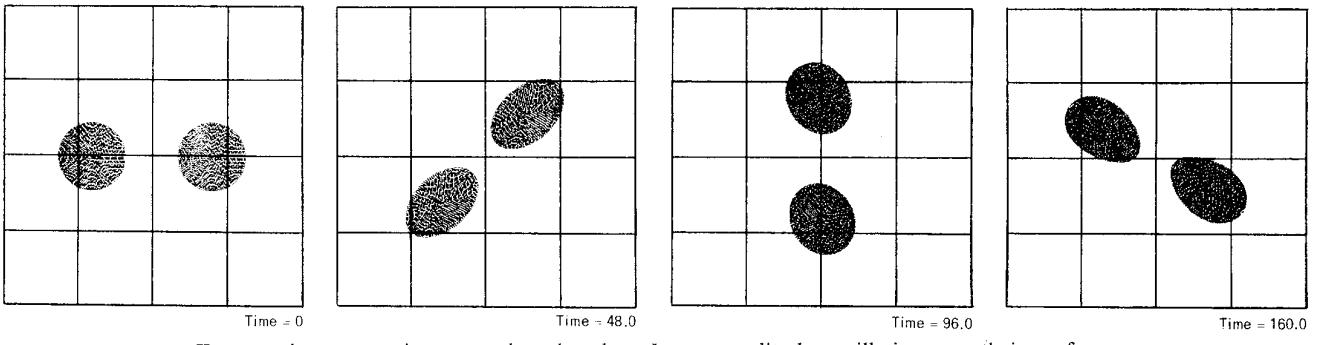

Two vortices precessing around each other. Large amplitude oscillations on their surfaces.

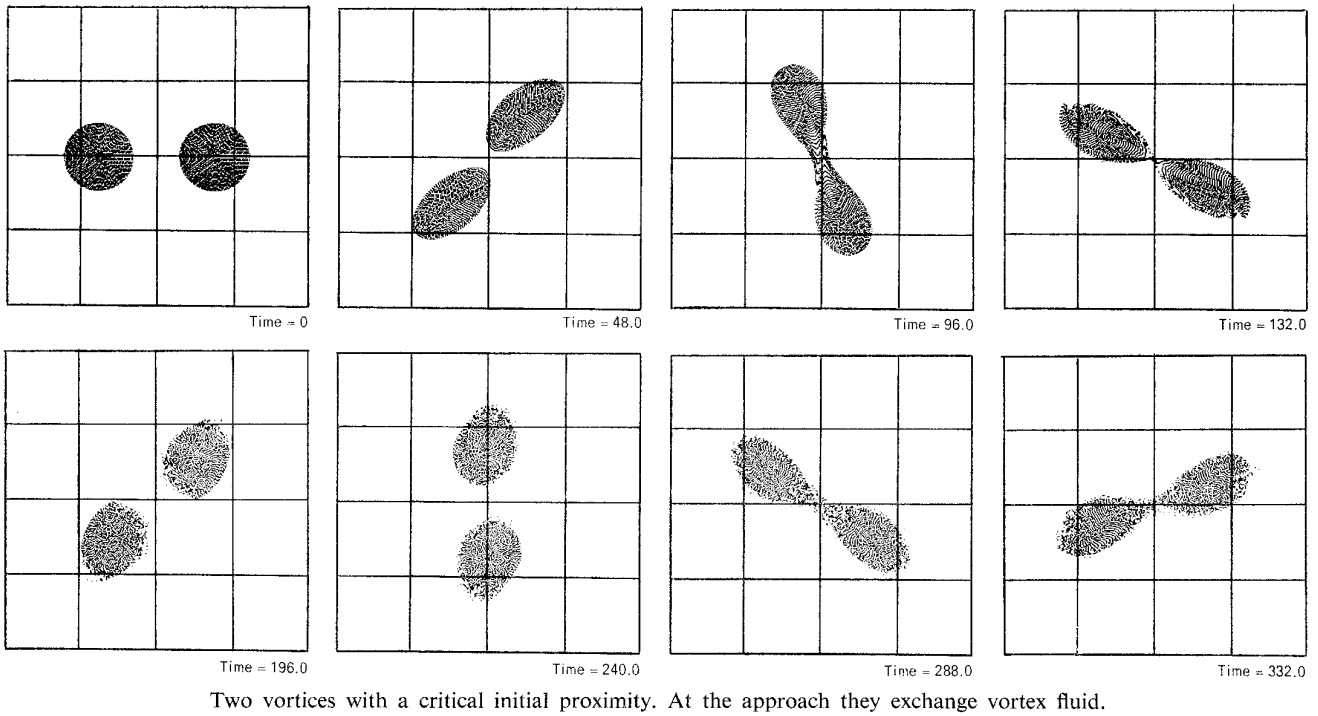

Two vortices with a critical initial proximity. At the approach they exchange vortex fluid.

FIG. 6. The elementary interaction between two vortices of the same polarity.

method introduces a radial velocity component which changes the circular particle orbits by up to 1% during half a rotation period, or roughly the amount corresponding to the amplitude of a_4 at $t = T/2$.

The seven experiments on the test model show that the most significant numerical error arises from the anisotropic CIC—interpolation of velocities given by Eq. (15). The truncation errors associated with the finite difference forms have negligible influence on the growth of the azimuthal modes a_{4m} which slowly distort the circular surface of the vortex. The only way to remove this anomaly is either to adopt a more complex interpolation algorithm which produces an isotropic velocity field from a point vortex (r-dependence only) or to employ a different mesh structure (for example a hexagonal or triangular mesh). Interpolation algorithms much more costly than the CIC method have recently been developed by Hockney *et al.* [23] for applications in plasma simulations where isotropic force fields from single particles are required.

7. ADVANTAGES AND DEFICIENCIES OF PARTICLE APPROACH

Two questions that inevitably arise from the foregoing discussion are: How useful is the particle model for a further study of hydrodynamics? And how does it compare with other numerical techniques?

The answer to the first question is based on our experience from a series of numerical simulations on a variety of hydrodynamic problems (see Figs. 5 and 6). The particle model has proved useful and reliable within a time range that naturally depends on what accuracy is needed and what kind of distribution is required. Good agreement has been achieved between theory and a number of numerical results [17, 18]. For a given flow problem that can be described analytically in the linear regime we can by comparing theory and experiment acquire a quantitative understanding of how the inaccuracies are related to the length of the time integration. In most of the cases that we have encountered the prominent part of the evolution takes place before the accumulation of errors can distort the result. For example, in studies of the interaction between vortices [24] the picture of evolution is almost complete within 3, 4, or 5 periods of rotation of a single vortex, limiting the anomalous growth of azimuthal modes studied in this paper to, say, 5–6%.

The main alternative to our method seems to be a mesh method like the one used by Fromm and Harlow [25] or by Zabusky and Deem [26], which is subject to conditions for numerical stability analogous to those outlined in [15] but causes vorticity to diffuse very quickly so that pictures such as those of Figs. 5 and 6 could not be obtained in this way. During the development of our technique the accurate graphical display of the particle positions seemed an attractive feature, and we were also attracted by the particle method when it became clear how to optimize the equations of motion for particles [16] so that the amount of computer time required for either method is much the same.

8. CONCLUSION

We have presented a particle model which simulates the motion of a continuous hydrodynamic fluid. We have shown how the numerical scheme like any other finite difference formulation contains certain anomalies. Our test problem has, however, proved that the approximations made will not affect the results seriously over a timescale appropriate for a study of many hydrodynamic flows (see Figs. 5 and 6).

ACKNOWLEDGMENTS

I am indebted to Dr. K. V. Roberts, who has been deeply involved in all phases of this work from its inception and who has carefully read and criticized the manuscript. I would also like to thank Dr. G. Rowlands and Dr. J. B. Taylor for their helpful comments and discussions.

REFERENCES

1. F. H. Harlow, *Numerical Methods for Fluid Dynamics, an Annotated Bibliography*, Los Alamos Report LA-4821 (1970).
2. R. W. Hockney, *J. Assoc. Comput. Mach.* **12,** 95 (1965).
3. R. W. Hockney, in *Methods of Computational Physics, Vol. 9* edited by B. Alder, S. Fernbach, and M. Rotenberg (Academic Press, New York, 1970).
4. J. P. Christiansen and K. V. Roberts, Paper 40 in *Proceedings of the Conference on Computational Physics, Culham Laboratory, July 1969*. [Available from HMSO]
5. B. Alder, S. Fernbach, and M. Rotenberg, Eds., *Methods of Computational Physics, Vol. 9* (Academic Press, New York, 1970).
6. H. L. Berk, C. E. Nielsen, and K. V. Roberts, *Phys. Fluids* **13,** 980 (1970).
7. J. B. Taylor and B. McNamara, *Phys. Fluids* **14,** 1492 (1971).
8. J. A. Byers, *Phys. Fluids* **9,** 1038 (1966).
9. R. H. Levy and R. W. Hockney, *Phys. Fluids* **11,** 766 (1968).
10. C. K. Birdsall and D. Fuss, Report UCRL-50002-68 (1968).
11. F. H. Abernathy and R. E. Kronauer, *J. Fluid Mech.* **13,** 1 (1962).
12. A. J. Chorin, *J. Fluid Mech.* **57,** 785 (1973).
13. C. K. Birdsall and D. Fuss, *J. Comp. Phys.* **3,** 494 (1969).
14. J. P. Christiansen and R. W. Hockney, *Comp. Phys. Comm.* 2 (1971).
15. J. P. Christiansen, Culham Report CLM-R106 (1970). [HMSO].
16. J. P. Boris and K. V. Roberts, *J. Comp. Phys.* **4,** 552 (1969).
17. J. P. Christiansen, *The Non-linear Dynamics of Vortex Flows by Numerical Methods*, Ph.D. dissertation, University of Warwick (1973).
18. J. P. Christiansen and J. B. Taylor, *Plasma Physics* **15,** 585 (1973).
19. H. Lamb, *Hydrodynamics*, 6th ed. (Cambridge Univ. Press, London/New York, 1932).
20. A. B. Bassett, *Hydrodynamics, Vol. 2* (Dover, New York, 1961).

21. T. Ling and C. Tung, *Phys. Fluids* **8,** 1039 (1965).
22. G. Morikawa and E. V. Swenson, *Phys. Fluids* **14,** 1058 (1971).
23. R. W. Hockney, S. P. Goel, and J. W. Eastwood, *J. Comp. Phys.* **14,** 148–158 (1974).
24. J. P. Christiansen and N. J. Zabusky, *J. Fluid Mech.* **61,** 219–243 (1973).
25. J. E. Fromm and F. H. Harlow, *Phys. Fluids* **6,** 975 (1963).
26. N. J. Zabusky and G. S. Deem, *J. Fluid Mech.* **47,** 353 (1971).